

# Evolutionary Consequences of Many-to-One Mapping of Jaw Morphology to Mechanics in Labrid Fishes

Michael E. Alfaro,<sup>1,2,\*</sup> Daniel I. Bolnick,<sup>1,3</sup> and Peter C. Wainwright<sup>1</sup>

1. Section of Evolution and Ecology, University of California, Davis, California 95616;

2. School of Biological Sciences, Washington State University, Pullman, Washington 99164;

3. Section of Integrative Biology, School of Biological Sciences, University of Texas, Austin, Texas 78712-0253

Submitted July 2, 2004; Accepted January 10, 2005;  
Electronically published April 4, 2005

Online enhancement: Mathematica notebook.

---

**ABSTRACT:** Many physiological traits consist of two hierarchically related levels: physical structures and the emergent functional properties of those structures. Because selection tends to act on the emergent functional traits, the evolution of structural phenotypes will depend on the nature of the form-function relationship. Complex physiological or biomechanical traits are often characterized by many-to-one mapping: numerous structural phenotypes can yield equivalent functions. We suggest that this redundancy can promote the evolution of phenotypic diversity, and we illustrate this effect with a combination of empirical and analytical studies of a complex biomechanical trait, the four-bar linkage found in the jaws of labrid fishes. We show that labrid jaws are subject to many-to-one mapping of form-to-jaw mechanical properties but that some mechanical types have higher levels of morphological redundancy than others. This variation in redundancy has affected the diversity and distribution of labrid jaw shapes: labrid species are disproportionately concentrated around functional traits with higher potential for redundancy. Many-to-one mapping can also mitigate evolutionary constraints imposed by mechanical trade-offs by allowing a species to simultaneously optimize multiple functional properties. Many-to-one mapping may be an important factor in generating the uneven patterns of diversity in physiological traits.

**Keywords:** biomechanics, physiology, four-bar, Labridae, neutral evolution, functional equivalence.

---

\* Corresponding author; e-mail: alfaro@wsu.edu.

Am. Nat. 2005. Vol. 165, pp. E140–E154. © 2005 by The University of Chicago. 0003-0147/2005/16506-4051\$15.00. All rights reserved.

Comparative biologists have long recognized that physiological and morphological diversity are unevenly distributed among lineages and have sought to identify the underlying causes. Workers have examined extrinsic causes, such as access to novel environments (e.g., Grant 1986; Baldwin and Sanderson 1998; Farrell 1998; Marvaldi et al. 2002) and the role of ecological opportunity (Schluter 2000). Intrinsic novelties are also thought to influence physiological diversification. The key innovation hypothesis posits that novel structural or functional acquisitions promote physiological and/or functional diversification (e.g., Ostrom 1979; Farrell 1998; Middleton and Gatesy 2000). Trait duplication and decoupling is a second mechanism that has been proposed to lead to physiological diversification (e.g., Liem and Osse 1975; Schaefer and Lauder 1986; Lauder 1990; Schaefer and Lauder 1996; Friel and Wainwright 1998). Vermeij's (1973) hypothesis, which increases in complexity—the number of independent parameters to specify a design—to generate greater potential morphospace and diversity, is a third.

Functional redundancy is another very general phenomenon that can facilitate diversification, although it is more commonly invoked to explain patterns of molecular evolution. Redundancy occurs when a number of different underlying structures can produce the same emergent functional property of a trait. For example, the amino acid structure of an enzyme might map redundantly to its catalytic ability in that similarly functioning enzymes can differ at some amino acid sites. The concept of multifunctionality (Zuckerandl 1997) and its bearing on evolutionary dynamics have been discussed at length with respect to selectively neutral amino acid substitutions (Ohta 1992) and 12S rRNA secondary structure (Schuster et al. 1994; Fontana and Schuster 1998; Schuster and Fontana 1999; Stadler et al. 2001). Importantly, almost any genotype-phenotype relationship implies a redundant (or many-to-one) mapping of genotype to phenotype (Stadler et al. 2001), and redundancy, in turn, may strongly affect the tempo and mode of evolutionary diversification (Schuster et al. 1994; Zuckerandl 1997; Fontana and

Schuster 1998; Schuster and Fontana 1999; Stadler et al. 2001).

In an analogous fashion to the molecular traits described above, many physiological structures exhibit a pattern in which multiple combinations of underlying parts can give rise to traits with similar mechanical, physiological, or performance values (Wainwright et al. 1976; Lewontin 1978; Taylor and Weibel 1981; Norberg 1994; Koehl 1996; Kovach 1996; Nishikawa 1999). For example, muscles with similar tension-producing capacities can be constructed with disparate fiber lengths, fiber orientations, and specific tensions (Powell et al. 1984). At the level of whole-organism performance, lizards may achieve similar levels of jumping ability with many different combinations of muscle size and hindlimb dimension (Toro et al. 2004). Thus, many-to-one mapping of form to function also characterizes the relationship between physiological phenotype and higher levels (or emergent properties) of the phenotype (Lewontin 1978).

Given that redundancy appears to be a common property of many physiological systems, an understanding of the evolutionary consequences of many-to-one mapping might improve studies of diversity and ecology. Redundancy enables structural change to be functionally (and hence selectively) neutral and imparts nonlinearity to the relationship between change at the functional level of a trait and change at the underlying structural level. Both of these properties might be expected to influence the evolutionary behavior of a trait. Form-function maps might be used to distinguish between functional diversification within a clade and morphological diversification, key issues in the study of adaptive radiation. Study of form-function mapping also might help identify conditions under which morphological variation is expected to have an exceptionally weak correlation with emergent levels of design, possibly shedding additional light on the issues surrounding the use of morphology as a proxy for ecology (Gatz 1979; Winemiller 1991; Ricklefs and Miles 1994; Lovette et al. 2002).

As a step toward understanding the evolutionary consequences of many-to-one mapping for physiological traits, we have undertaken a study of the relationship between morphological and mechanical evolution in the four-bar linkage (Hulsey and Wainwright 2002; Alfaro et al. 2004), a biomechanical trait found in the skulls of labrid fishes (Wainwright et al. 2004). Four-bars are exceptionally well suited to studying form-function evolution because the structural phenotype can be summarized by three quantitative variables and an emergent mechanical property of functional importance can be precisely calculated from the morphology. Previously, using simulation and numerical techniques, we found that redundancy can partially decouple mechanical and morphological evolution

and promote morphological diversification even in the face of selection for functional equivalence (Alfaro et al. 2004).

Here we extend our earlier work by developing an analytic approach to the study of the map between morphology and mechanics. Within the four-bar framework, we ask what the intrinsic bounds to mechanical evolution are and if the pattern of mechanical diversity in labrids reflects these boundaries. We also ask how labrids have distributed themselves throughout theoretical morpho- and mechanospaces. Finally, we use this system to illustrate how redundancy can promote functional diversification and mitigate against trade-offs in the face of disparate functional demands. Although our work focuses on a single functional trait in fish jaws, common vertebrate performance traits such as sprint speed, jump distance, bite force, and suction pressure typically exhibit redundancy in the map of underlying parts to functional variables. Thus, we expect that the principles that emerge from the study of this system will have broad applicability for a wide range of biomechanical, physiological, and behavioral characters.

## Methods

### *The Labrid Four-Bar Mechanism*

In contrast to humans and other mammals in which the lower jaw is the single freely articulating element of the skull, fish heads are highly kinetic and contain a large number of mobile joints. Motion of many skeletal elements of the fish skull has been modeled using lever theory, borrowed from mechanical engineering. The four-bar is a mechanical lever system that describes motion in the oral jaws of labrid fishes (fig. 1; Westneat 1990; Muller 1996; Wainwright et al. 2004). It functions to transmit force and motion through a series of four skeletal elements connected in a loop. One property of the four-bar that makes it especially tractable for mechanical analysis is that the system possesses a single degree of freedom (meaning that for any given angle between two links, all remaining angles of the mechanism are determined). Thus, rotation applied to the lower jaw link results in movement of the nasal and maxilla links (relative to the fixed link) in a deterministic way (fig. 1).

One key mechanical property of the system is the maxillary kinematic transmission coefficient (maxillary KT). Analogous to the inverse of a lever mechanical advantage, maxillary KT describes the amount of angular rotation of the maxillary bone for a given amount of lower jaw rotation that in turn is thought to control protrusion of the premaxilla (Westneat 1990). This functional property can be calculated for any given morphology using simple trigonometry (app. B). Maxillary KT has been shown to have

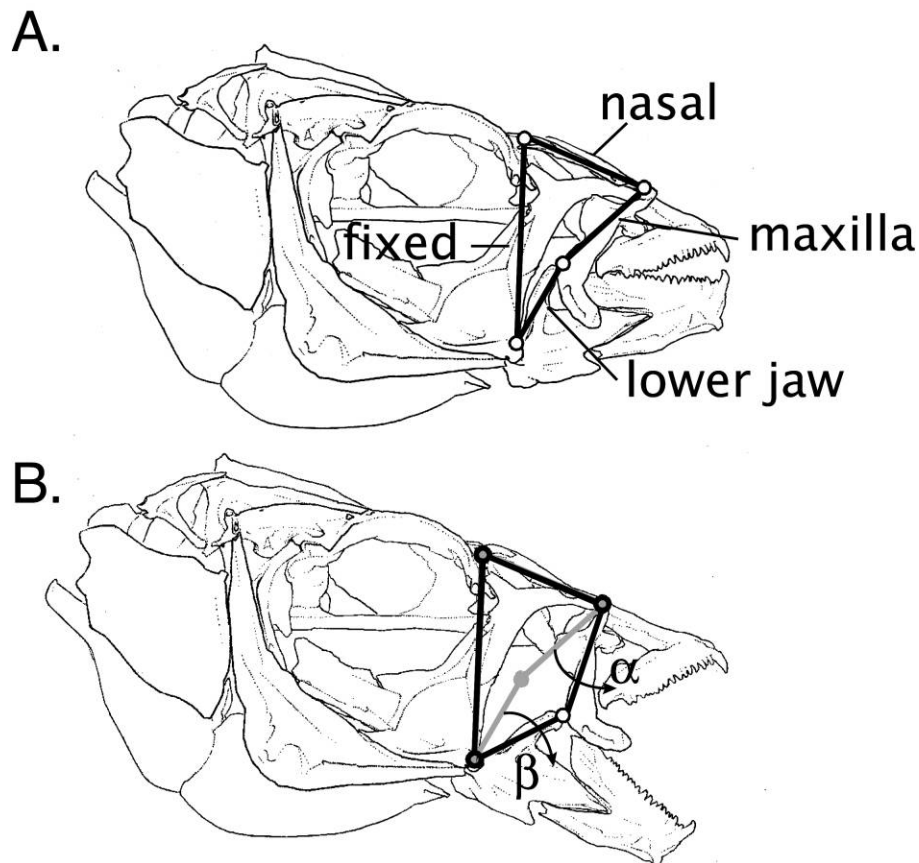


**Figure 1:** Illustration of the labrid oral jaws four-bar linkage in (A) closed and (B) open position. Four bony elements (*fixed*, *lower jaw*, *maxilla*, *nasal*) are connected at mobile joints to form a loop. During mouth opening, downward rotation of the lower jaw is translated to the maxilla, which is rotated anteriorly. A mechanical property of this system, the maxillary kinematic transmission coefficient (maxillary KT =  $\alpha/\beta$ ) describes the amount of maxillary rotation ( $\alpha$ ) per degree of lower jaw rotation ( $\beta$ ).

a significant correlation with ecology: species that feed on evasive prey tend to have higher maxillary KTs, and those taking hard-shelled prey have lower maxillary KTs (Westneat 1995; Wainwright et al. 2004). Maxillary KT varies with four-bar shape in a nonlinear and redundant fashion, meaning that there are many possible combinations of links that produce the same maxillary KT (Hulsey and Wainwright 2002; Alfaro et al. 2004).

Maxillary KT is sensitive to the starting and input angles of the lower jaw, although these parameters are typically less important than the lengths of the links (Hulsey and Wainwright 2002). For these reasons, we fix starting angle and input angle to be  $30^\circ$  for all calculations of maxillary KT in this study. These numbers reflect biologically relevant values for labrids (Westneat 1990). By setting these two variables to be constants and by expressing the length of the nasal, lower jaw, and maxillary links as a proportion

of the fixed link (four-bar mechanics are size independent), we are able to describe the structure of the four-bar jaw linkage in a three-dimensional morphospace that can be readily visualized. Had we allowed these angles to vary, our analysis would have been more difficult to describe (being five-dimensional rather than three-dimensional) but would have shown similar dynamics to those discussed here since there would have been even higher levels of redundancy.

Although we define maxillary KT as the function of the four-bar for the purposes of this study, in reality jaw function in labrids will depend on many structures and properties beyond those considered here. Thus, fish with mechanically equivalent four-bars are not necessarily expected to have functionally equivalent jaws. We do not believe that this limitation invalidates our approach because the framework we develop could be extended to incorporate

additional structural elements in order to examine broader or more emergent functional properties.

#### *Theoretical Number of Mechanical Solutions*

We used a simulation approach to discover the relative number of morphological solutions for values of maxillary KT across biologically plausible four-bar shapes. Using a data set that included measurements from an earlier study (Wainwright et al. 2004) along with new measurements (table A1), we defined two labrid morphospaces, a “shoebox” and a spheroid. To create the shoebox, we determined the minimum and maximum lengths observed for each of the four-bar elements in the 122 species in our data set. The minimum and maximum observed lengths of these elements ([minimum, maximum], expressed as a proportion of the fixed link; see above) constituted the lower and upper bounds on the theoretical morphospace: lower jaw  $\in [0.23, 0.68]$ , nasal  $\in [0.34, 0.54]$ , maxilla  $\in [0.32, 0.73]$ .

We wrote a computer program in LISP to calculate the maxillary KT for every four-bar within this morphospace. Starting with a four-bar with dimensions fixed link = 1.0, lower jaw, nasal, and maxillary links equal to their minimum values (above), and a starting angle between the lower jaw and the fixed link of 30°, the program determined the maxillary KT given 30° of input rotation. The length of the lower jaw was then incremented by 0.01, and maxillary KT was recalculated. The program repeated the process of incrementing a length by 0.01 and recalculating maxillary KT until all possible four-bars had been evaluated ( $N = 164,300$ ).

The four-bar samples produced by this procedure were spaced evenly within a box-shaped volume defined by the minimum and maximum lengths of each link observed in the labrids. However, we suspected that this theoretical morphospace would include large regions unoccupied by living species, particularly around the periphery. To shave away these empty corners of the shoebox, we also defined a spheroidal morphospace using a series of bivariate plots of link length (lower jaw by nasal, lower jaw by maxilla, maxilla by nasal). Starting with the lower jaw by nasal plot, we constructed a convex hull (the smallest convex polygon containing all of the labrids) using JMP 5.01 (SAS 2002) and eliminated all simulated four-bars that fell outside of it. We repeated this procedure for the other two combinations of links, defining a second morphospace that represents a three-dimensional convex hull around the cloud of labrids in the lower jaw, nasal, and maxilla morphospace. This cloud contained 35,306 four-bars, substantially fewer than the shoebox space, revealing labrids to be nonuniformly distributed in the shoebox morphospace. We compared the variance of the empirical distri-

bution of maxillary KTs in 122 labrids to variance in maxillary KT in the shoebox and spheroid morphospaces using an *F*-test.

Given the large size of the theoretical sample, we expected to have great statistical power to discriminate between the theoretical and empirical distributions. To test if parameters of the empirical data differed significantly from randomly drawn samples from the theoretical space, we performed a resampling analysis. We generated replicate data sets of 122 taxa by drawing randomly from each theoretical distribution of maxillary KT. For each replicate, we log transformed the data and calculated the shape and scale parameters of the distribution to create null distributions. The empirical shape and scale parameters were compared to these null distributions to determine if they differed significantly from random expectation.

#### *Mathematical Modeling*

The relationship between the geometry of the four-bar and its maxillary KT can be described using a series of trigonometric equations (app. B). We used Mathematica 4.2 (Wolfram Research 2002) to solve for all possible four-bar morphologies that would produce a given value of maxillary KT within the wrasse-bounded morphospace described above. We visualized functionally equivalent morphologies by plotting contours through all points with a given maxillary KT.

#### *Multiple Functional Demands*

Many complex traits are known or thought to be subject to disparate functional demands. For example, the bony elements of the four-bar are conspicuous components of the skull and almost certainly influence functional traits such as maximum mouth gape, maximum buccal expansion, and hydrodynamic profile. Unfortunately, we currently lack an explicit model that ties four-bar morphology to multiple known functions. In the absence of such a model, we extended our four-bar framework to include a second mechanical property with no known functional or ecological significance. We defined nasal KT as the ratio of rotation of the nasal link to that of the lower jaw and used it, along with maxillary KT, to theoretically explore how the intrinsic relationships between morphology and multiple functions might influence the evolution of a complex trait subject to multiple functional demands. We used Mathematica to plot the intersection of two nasal KT contours (0.0, representing a four-bar in which the nasal link does not move while the maxilla rotates, and 0.55, representing four-bars with relatively extreme nasal movement), with the maxillary KT = 0.8 contour to explore how these properties relate to one another. We also ex-

plored the diversity of nasal KT in living labrids with maxillary KTs of approximately 0.8.

We used a randomization test to examine whether a constraint imposed by a secondary function reduced four-bar morphological diversity. We compared the morphological variance found in six species with both a maxillary  $KT = 0.8 \pm 0.05$  and a nasal  $KT = 0.55 \pm 0.05$  to the variance found in species with the same maxillary KT but unconstrained nasal KT. We created the null distribution by repeatedly ( $N = 1,000$ ) drawing random samples of six species with maxillary  $KT = 0.8 \pm 0.05$  from the labrid data set and computing the sum of the variance found in each link for the replicate. Multiple functional demands were interpreted as significantly reducing morphological solutions if the variance from the constrained sample fell within the lower 5% tail of the null distribution.

### Results

Morphological solutions to maxillary KT within the shoebox morphospace are approximately lognormal distributed ( $\mu = -0.22$ ,  $\sigma = 0.50$ ) with a median value of 0.79 (fig. 2A). Ninety-five percent of all possible morphologies produce a maxillary KT of 2.1 or less. The minimum KT possible is 0.06, and the maximum is 3.82. The morphological solutions within the spheroidal morphospace are similarly distributed ( $\mu = -0.20$ ,  $\sigma = 0.32$ ), with a median KT of 0.80, a minimum KT of 0.41, a maximum KT of 2.3, and 95% of four-bars producing a maxillary KT of 1.6 or less. The empirical samples are also approximately lognormal distributed ( $\mu = -0.22$ ,  $\sigma = 0.27$ ), with a median KT of 0.80 (fig. 2B). The maximum observed KT was 1.95, and the minimum KT was 0.45. The variance of the empirical data is lower than that of the shoebox samples ( $F = 3.73$ ,  $df = 164,300, 122$ ,  $P < .001$ ). It is also lower than theoretical samples within the spheroid morphospace ( $F = 1.38$ ,  $df = 35,306, 122$ ,  $P < .018$ ). Bootstrapping analysis underscored the  $F$ -test result, showing that the empirical sample variance is significantly smaller than the theoretical ( $P < .001$  for shoebox and spheroid). The empirical mean, however, does not differ significantly from either theoretical sample ( $P = .64$  for shoebox,  $P = .57$  for spheroid).

Contours of mechanical equivalence are continuous, highly curved, and irregularly spaced surfaces within the labrid morphospace (fig. 3A). As predicted by our numerical simulations above, the maxillary  $KT = 0.8$  iso-curve has the largest surface area in this space, with more extreme KT contours becoming progressively smaller. Twenty-two labrid species in our sample possess a maxillary  $KT$  of  $0.8 \pm 0.05$  (fig. 3B). Despite occupying a relatively restricted portion of the possible morphospace,

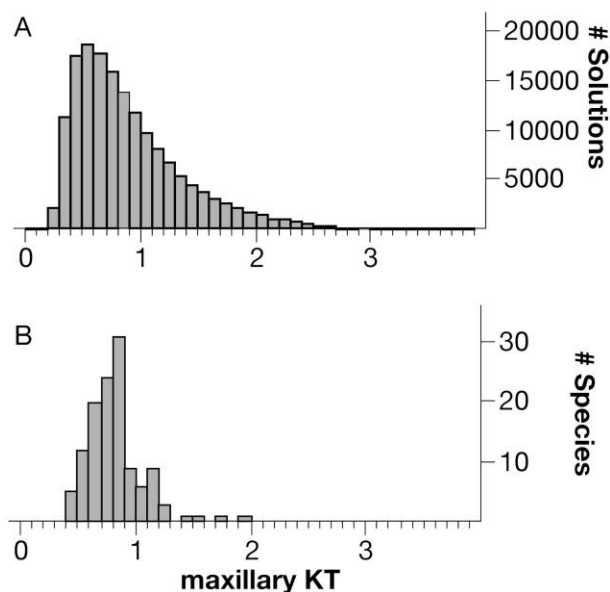


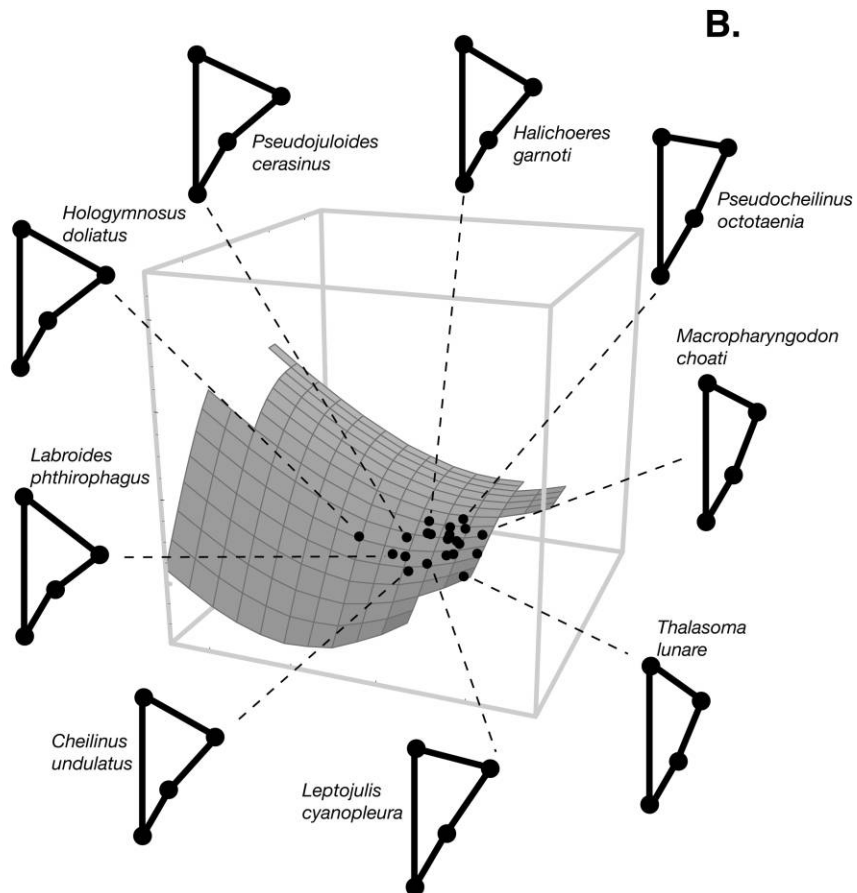
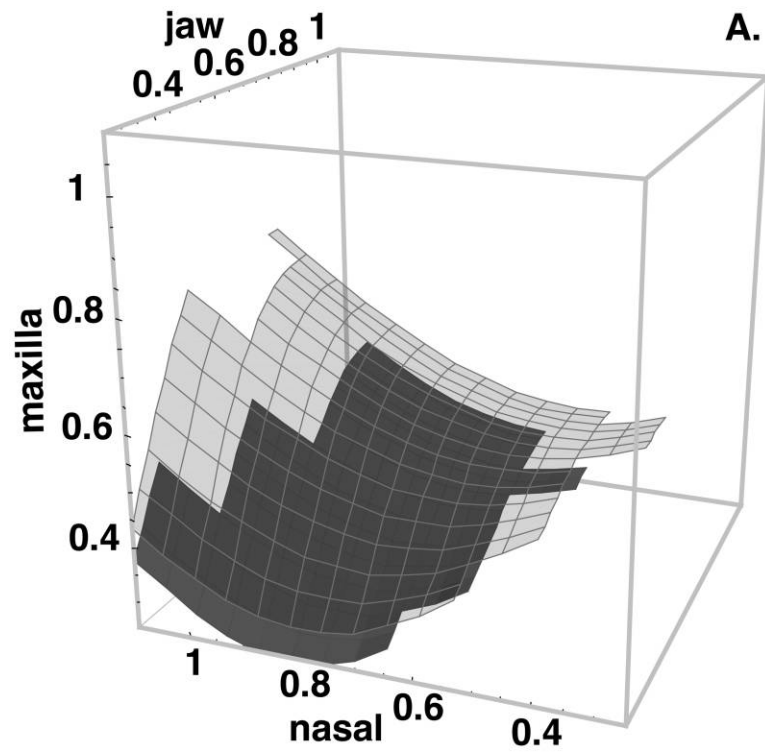
**Figure 2:** Redundant morphological solutions for mechanical types. *A*, Theoretical number of morphological solutions for four-bars with equivalent maxillary KTs across biologically realistic link lengths within the shoebox morphospace (see text). Theoretical distribution is approximately lognormal with scale ( $\mu$ ) =  $-0.22$  and shape parameter ( $\sigma$ ) =  $0.50$ . Median value of  $KT = 0.79$ . *B*, Distribution of maxillary KTs in 122 labrids. Empirical distribution is also approximately lognormal with similar mean ( $\mu = -0.22$ ) but smaller variance ( $\sigma = 0.24$ ). Empirical  $KT$  median value =  $0.80$ .

these species show a high degree of four-bar morphological diversity (fig. 3B).

Nasal  $KT$  contours are also highly curved and irregularly spaced and run roughly orthogonal to maxillary  $KT$  contours (fig. 4). Within the labrids sampled in this study, there is a significant positive correlation between these two mechanical properties ( $r^2 = 0.16$ ,  $F = 22.51$ ,  $df = 118$ ,  $P < .001$ ). Nevertheless, we found considerable diversity in nasal  $KT$ s among labrids with approximately equal maxillary  $KT$ s (fig. 5A). Within our sample, four-bar morphological diversity in labrids with similar maxillary  $KT$ s and nasal  $KT$ s is not significantly lower than four-bar diversity among labrids with similar maxillary  $KT$ s only ( $P = .13$ ), although the observed range of morphologies appears qualitatively to be less extreme (fig. 5B) than in unconstrained samples (fig. 5A).

### Discussion

Functional morphologists have long recognized that the relationship between morphology and mechanics can be nonlinear and that within a physiological system, there may be “more than one way to skin a cat” (Koehl 1996).



Despite the prevalence of these ideas within the fields of evolutionary morphology and physiology, there have been very few explicit attempts to understand how the intrinsic relationship between morphology and functional properties is expected to influence physiological evolution.

Our study reveals that the map of morphology to mechanics could influence physiological diversification in many ways. First, because solutions to functional problems may not be uniformly distributed in complex traits, the distribution itself might impose a kind of dynamic constraint on the evolution of morphological diversity across lineages. For example, in the labrid four-bar morphospace, there are a large number of possible morphologies that will produce a KT of approximately 0.8 (fig. 2). Therefore, under a scenario in which selection is acting at the level of mechanics, clades under selection for KT of 0.8 have the potential to evolve a high degree of morphological diversity. In contrast, clades under selection for high maxillary KT ( $>2.0$  for example) have reduced potential for morphological diversification simply because there are fewer morphological possibilities. Similarly, individual lineages under selection for extreme values of maxillary KT might be expected to have a greater chance of evolving morphologically convergent four-bars simply because there are only a small number of possible mechanical designs. In contrast, morphological convergence is far less likely to accompany mechanical convergence in lineages evolving toward maxillary KT = 0.8. Thus, an understanding of the morphology-function map might help identify the relative importance of intrinsic mechanical constraints on the evolution of morphological convergence.

Such an approach might also help explain patterns of ecological diversification. For example, it is intriguing to note that piscivores and planktivores are the rarer ecotypes within the Labridae (Wainwright et al. 2004), that these ecotypes are predicted to require the highest-KT jaws, and that there are relatively few high-KT solutions available to wrasses within the morphospace (fig. 2).

#### *Possible and Attained Jaw Forms*

Why do labrids appear to occupy only a small portion of the theoretical morphospace (fig. 3B)? The bounds of the KT = 0.8 surface in figure 3B are determined by two fac-

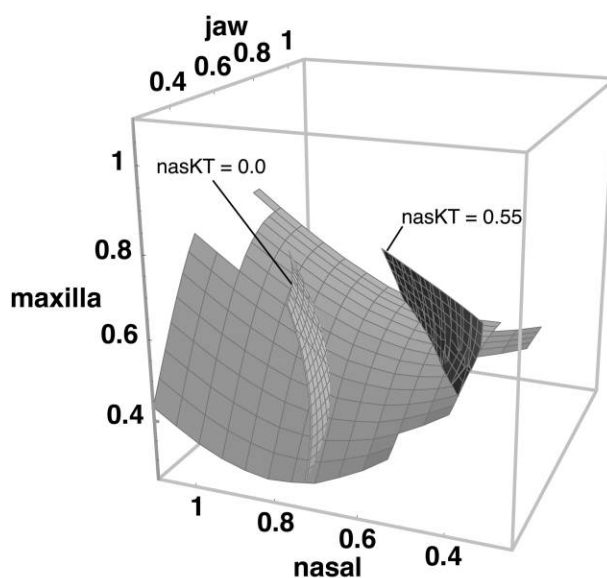


**Figure 4:** Redundant mechanical mapping allows simultaneous optimization of multiple emergent functions. Shown is the intersection of two isocurves of nasal KT (nKT),  $nKT = 0.0$  and  $nKT = 0.55$  with the mean maxillary KT (maxillary KT = 0.8) isocurve in the labrid four-bar morphospace. Intersections of these isocurves represent axes of four-bar morphological variation that are mechanically equivalent for two functional properties simultaneously.

tors. The first is the minimum and maximum values of the lower jaw, nasal, and maxillary links for all species (not just those of KT = 0.8). Thus, the unoccupied areas of the KT surface indicate that some species with higher or lower KTs have four-bar element lengths that fall outside the range of those found in species with maxillary KT = 0.8. A second bound on surface areas in this space is the functional constraint that the combination of links forms a functional four-bar. In figure 3B, the border on the lower right constitutes a hard edge in the space because of the physical requirement that the sum of the lengths of the lower jaw, nasal, and maxillary must exceed 1.0 to produce a working four-bar.

Given these constraints on the theoretical surface, the question remains why labrids are distributed across the KT = 0.8 surface in a nonuniform way. Why do wrasses with KT = 0.8 never evolve long nasals and short maxillas,

**Figure 3:** Contours of mechanical equivalence within the labrid morphospace. Axes show the lower jaw, nasal, and maxilla links expressed as a proportion of the fixed link. A, Maxillary KT = 0.8 (light gray) and maxillary KT = 1.0 (dark gray) contours. Any point along the contours describes the dimensions of a four-bar with the indicated maxillary KT. Maxillary KT = 0.8 represents the theoretically largest surface within the space. More extreme values of KT have smaller surface areas, indicating fewer possible morphological solutions. Although KT isocurves are highly nonlinear, contours near the median KT run roughly parallel to one another. B, Position of 22 labrids with maxillary KT =  $0.8 \pm 0.05$ . Despite occupying a relatively restricted portion of the theoretical morphospace, labrids with similar values of maxillary KT exhibit a high degree of diversity.

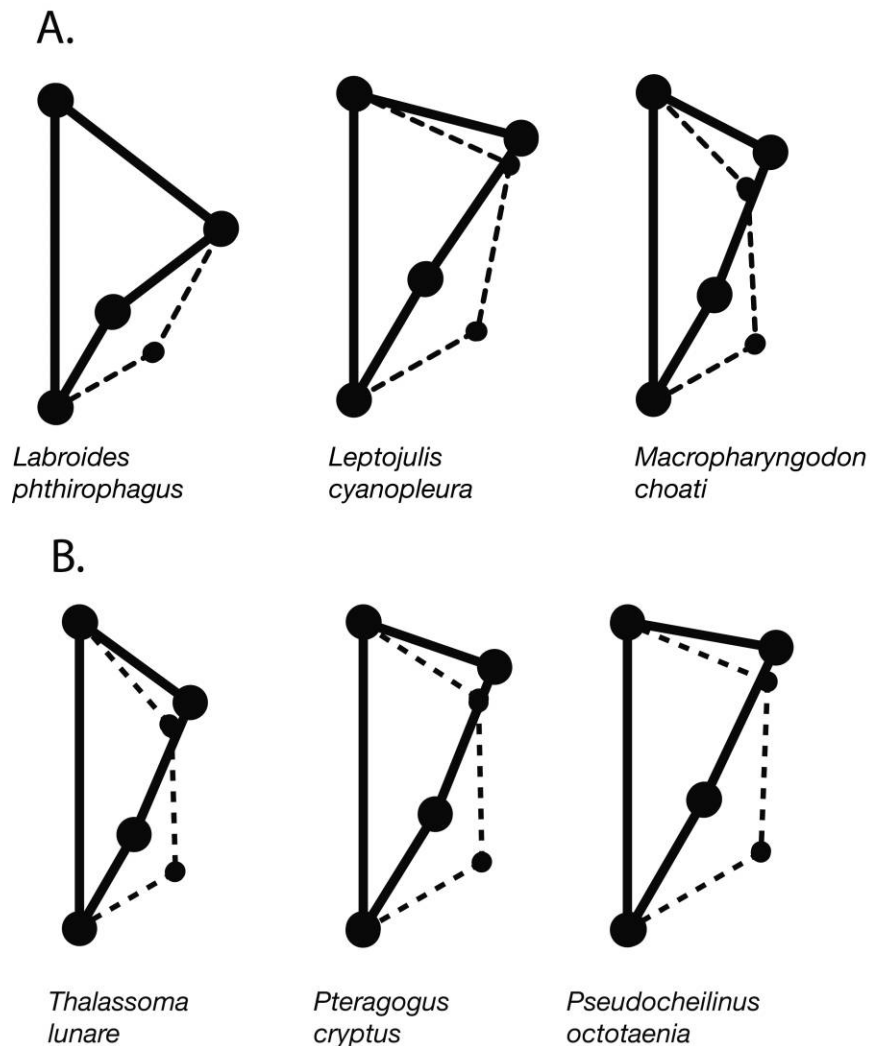


**Figure 5:** Redundant mapping of function to function. *A*, Within sampled labrids, nasal KT and morphology showed considerable variation among species with a similar value of maxillary KT. In the three species shown, maxillary KT equals  $0.8 \pm 0.5$ , and nasal KT ranges from 0.0 in *Labroides* to 0.6 in *Macropharyngodon*. *B*, Multiple functional demands do not necessarily constrain morphological diversity. Here three species with similar values of maxillary KT ( $0.8 \pm 0.05$ ) and nasal KT ( $0.55 \pm 0.05$ ) exhibit obvious morphological variation. Observed morphological diversity in the six species from our data set that satisfied both of these mechanical constraints was not significantly lower than the expected morphological diversity of six labrids randomly sampled with maxillary KT = 0.8 and without respect to nasal KT (see text). Four-bar starting (*solid lines*) and ending (*dashed lines*) conformations are illustrated.

for example? One intriguing possibility concerns the evolutionary stability of the contours themselves. Although every point on a functional contour is, by definition, mechanically identical, they are not all identically buffered against mechanical change. Minor morphological change will have differential effects on mechanics depending on the position along the contour. This is another way of saying that the slope of steepest descent to an adjacent contour varies. Since populations vary in the length of their links, one hypothesis is that the observed distribution

represents the portion of the 0.8 contour in which population-level variation will have a relatively small effect on mechanics and the uninhabited areas represent forms in which mechanics change sharply with changes in morphology.

The stability of functional contours might also influence the degree of population-level morphological variation present in high- and low-KT lineages. For example, our model suggests that high-KT contours experience greater mechanical change per unit of morphological change than



low-KT contours (M. E. Alfaro, unpublished data). Thus selection on high-KT lineages might be expected to reduce the amount of morphological variation relative to low-KT lineages. Reduced morphological variation in turn could profoundly influence the evolutionary behavior of high-KT lineages versus low-KT lineages. Future work on within-population variation in link length will allow these and other hypotheses to be examined in greater detail.

#### *Complexity, Multiple Functions, and Diversity*

The form-function map can have a strong influence on the evolutionary dynamics of morphological units that belong to multiple functional traits. To illustrate this point, we consider a largely theoretical example of the evolution of underlying morphology and maxillary and nasal KT. Despite the lack of functional significance for nasal KT, we feel that this discussion is justified because the conceptual points we raise should be broadly applicable to any system in which morphology maps to multiple functions.

Given the elements of the four-bar (fixed, lower jaw, nasal, and maxillary links) and that two functional properties of the system (maxillary and nasal KT), we first consider a hypothetical scenario with no functional redundancy. In other words, every unique four-bar shape maps to a single value of maxillary KT and a single value of nasal KT. Figure 6A shows one example of the pattern of diversification that might be found within a clade in maxillary and nasal KT under such a scenario. The important point in this case is not the positive relationship between the two measures. Rather, it is that the number of possible combinations of maxillary KT and nasal KT is severely constrained. Without redundancy, functional diversification within this clade will be relatively low. In contrast, if redundant mapping of maxillary KT to nasal KT is possible, then functional diversification within a clade may be high because a greater number of combinations of maxillary and nasal KT values is possible (fig. 6B).

Perhaps more importantly, one-to-one mapping should severely constrain evolutionary change in traits with multiple functions, while redundant systems should be less constrained. Consider a system in which nasal and maxillary KT map one-to-one (fig. 6A), and assume a population with maxillary KT of 0.8 and nasal KT of 0.5. Furthermore, assume that these are selectively optimal values for the current conditions. If new conditions continue to favor maxillary KT = 0.8 but also a nasal KT of 0.0, the population will be unable to evolve a form that satisfies both functional demands because such a form does not exist. One-to-one mapping of morphology to multiple functions means that selection in this example will produce

a suboptimal phenotype for at least one of the functions. In contrast, in a redundant system such as that found within labrids (fig. 6B), this population could theoretically evolve a form that will simultaneously have the newly selected nasal KT and maintain the original nasal KT. Depending on the nasal KT and maxillary KT functional gradients, it is even possible that daughter populations would be able to maintain a maxillary KT of 0.8 as they evolved to the new nasal KT value.

The theoretical map of function to function can also be used to generate predictions about when trade-offs are likely to be important and when they are not. Although it is commonly thought that if a trait must accommodate disparate functions, some kind of trade-off between them must ensue, the maxillary KT–nasal KT example suggests that trade-offs need not occur over some ranges of functional values. For example, the shaded polygon in figure 6B indicates the realized functional space for nasal and maxillary KT values in living labrids. At high values of maxillary KT, there are relatively fewer possible nasal KT values than there are at maxillary KT values of 0.8. Thus, we might predict that functional trade-offs in this theoretical example would be more likely to occur when maxillary KT is selected to be high than when it is selected to be moderate. Data from other functional systems suggest that trade-offs may indeed display the kind of dynamic discussed here. For example, in anoles, horizontal jumping distance appears to map redundantly to flight time for submaximal distances but one-to-one at maximal jumping distance (Toro et al. 2004).

#### *Neutral Morphological Evolution and Physiological Diversification*

Previously, we showed that when selection is applied at the level of KT, many-to-one mapping can act as a mechanism for promoting diversification (Alfaro et al. 2004). The question of whether four-bar morphology in labrids has been driven primarily by selection at the level of lever mechanics or on the links themselves remains open. However, given both historical (Westneat 1995) and ahistorical (Wainwright et al. 2004) correlation of maxillary KT with diet, the hypothesis that selection has operated on maxillary KT is plausible. Given this possibility, the amount of morphological variation exhibited in taxa with similar values of maxillary KT (e.g., fig. 5A) is intriguing. In our sample, nine species in separate genera distributed throughout the labrid tree with disparate reconstructed ancestral KTs have evolved similar KTs (Westneat et al., forthcoming). Thus, the data suggest that mechanical convergence in the labrid four-bar is not accompanied by morphological convergence.

Could some of the morphological differences among

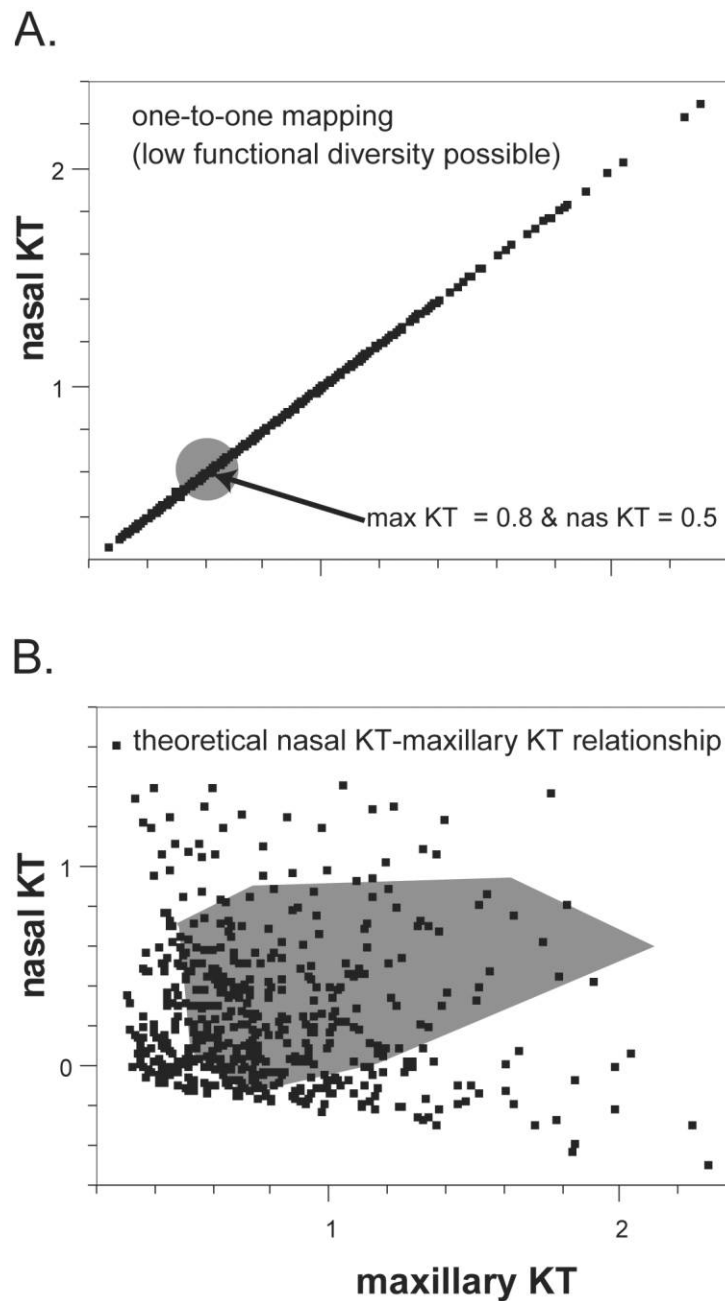


**Figure 6:** Mechanical diversification in redundant and nonredundant systems. *A*, Hypothetical nasal and maxillary KT values for a clade of 500 species where morphology maps one-to-one to these functional properties. Functional diversity within this clade is constrained to be low because few possible combinations of functional properties are possible. *B*, Nasal and maxillary KT values for 500 four-bars randomly sampled from the theoretical distribution of four-bars in the labrid morphospace (fig. 2A). Functional diversity within this clade is high owing to the larger possible number of combinations of nasal and maxillary KT values. Shaded polygon indicates the functional morphospace occupied by living labrids.

these lineages have arisen stochastically as they evolved under selection for function? Or has selection on secondary functions or on links directly produced the observed differences in four-bar form? Teasing apart these influences

will be difficult. The roles of drift and selection in molecular evolution continue to be debated, and nearly all of the difficulties that surround the identification of drift-induced molecular variation (e.g., Lynch 1984; Schluter

1996; Orr 1998; Phillips et al. 2001; Kelly 2003) will accompany studies of drift in phenotypic traits. However, when the map between form and function is analytically tractable, as it is in the four-bar system, it is possible to generate hypotheses about the patterns of morphological and mechanical variation that would be expected under various scenarios of selection on mechanics, morphology, or morphological drift, and these scenarios could then be tested using empirical data. For example, the hypothesis that selection on mechanics was the driving force behind four-bar shape evolution might be tested using a genotypic variance-covariance matrix for the four links in the population in question (which might be reasonably estimated using a phenotypic variance-covariance matrix) by using Lande's (1979) approach to multivariate trait evolution with the four-bar morphology mechanics map as the fitness landscape.

Neutral morphological evolution might be an important mechanism for enabling mechanical innovation in the

same way as evolution along neutral networks is thought to facilitate innovation in molecular systems (Zuckerandl 1997; Fontana and Schuster 1998; Schuster and Fontana 1999; Stadler et al. 2001). Given the ubiquity of many-to-one type mappings in physiological traits, continued investigation of the dynamics imposed on trait evolution by the interaction of selection and redundancy is warranted. Future studies will help determine if intrinsic relationships between morphology and function have played a major role in shaping patterns of diversification in complex physiological traits.

#### Acknowledgments

We thank A. Herrel and two anonymous reviewers for helpful comments on earlier versions of this manuscript. We also thank D. Hulsey and M. Turelli for helpful discussion and critical feedback during many phases of this project. This work was supported by a National Science Foundation grant (IBN-0076436) to P.C.W.

#### APPENDIX A

Table A1: Labrid species examined

Species	<i>N</i>	KT	Jaw	Nasal	Maxilla
<i>Anampses coeruleopunctatus</i>	3	.47	.37	.64	.64
<i>Anampses geographicus</i>	4	.55	.29	.67	.52
<i>Anampses melanurus</i>	3	.47	.32	.65	.63
<i>Anampses meleagrides</i>	4	.54	.34	.64	.60
<i>Anampses neoguinaicus</i>	3	.47	.31	.57	.58
<i>Anampses twistii</i>	1	.64	.32	.64	.49
<i>Bodianus anthioides</i>	4	.70	.40	.36	.57
<i>Bodianus axillaries</i>	4	.87	.43	.43	.51
<i>Bodianus diana</i>	5	.90	.50	.47	.52
<i>Bodianus loxozonus</i>	4	.74	.41	.42	.56
<i>Bodianus mesothorax</i>	3	.75	.44	.38	.56
<i>Bodianus perditio</i>	1	.62	.40	.39	.62
<i>Cheilinus chlorourus</i>	6	.92	.43	.48	.48
<i>Cheilinus fasciatus</i>	3	.75	.42	.50	.56
<i>Cheilinus oxycephalus</i>	4	1.17	.50	.47	.47
<i>Cheilinus trilobatus</i>	4	.79	.39	.48	.51
<i>Cheilinus undulates</i>	3	.75	.37	.61	.50
<i>Cheilio inermis</i>	9	.65	.43	.92	.59
<i>Choerodon anchorago</i>	3	.59	.31	.48	.53
<i>Choerodon cephalotes</i>	3	.54	.31	.57	.56
<i>Choerodon cyanodus</i>	3	.64	.35	.48	.54
<i>Choerodon fasciatus</i>	7	.80	.37	.43	.49
<i>Choerodon graphicus</i>	3	.62	.35	.44	.57
<i>Choerodon jordani</i>	6	.62	.38	.50	.60
<i>Choerodon schoenleinii</i>	4	.66	.34	.52	.51
<i>Choerodon sugillatum</i>	3	.54	.38	.48	.63
<i>Choerodon venustus</i>	3	.53	.30	.58	.57
<i>Choerodon vitta</i>	3	.51	.33	.46	.62
<i>Cirrhilabrus condei</i>	1	1.25	.49	.51	.55

Table A1 (Continued)

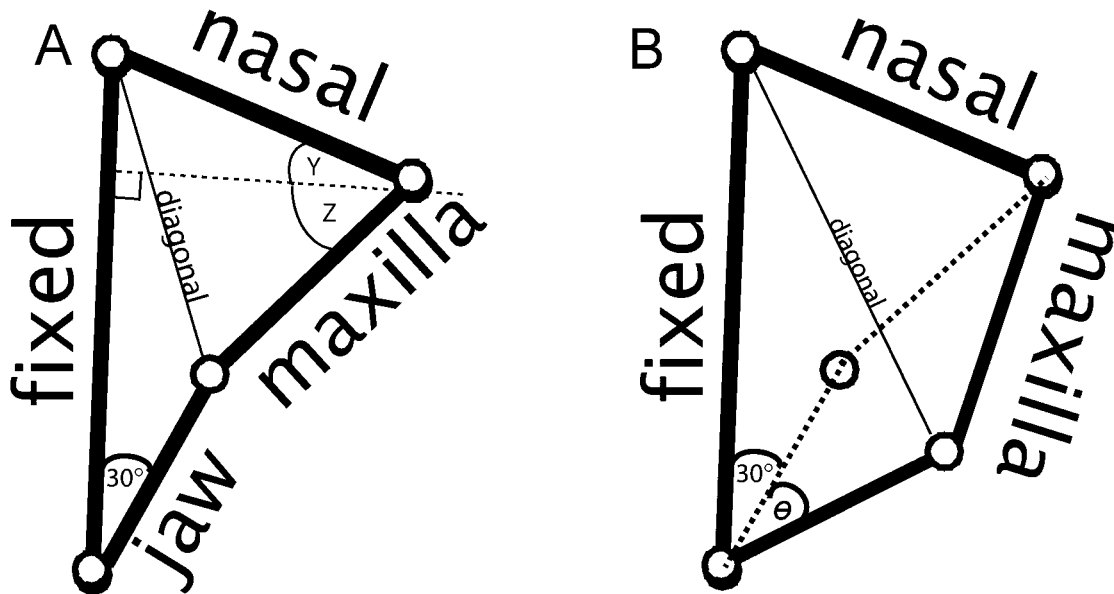
Species	N	KT	Jaw	Nasal	Maxilla
<i>Cirrhilabrus cyanopleura</i>	6	1.09	.51	.48	.47
<i>Cirrhilabrus exquisitus</i>	4	.98	.51	.45	.54
<i>Cirrhilabrus laboutei</i>	7	1.18	.51	.47	.47
<i>Cirrhilabrus lineatus</i>	7	1.17	.51	.45	.48
<i>Cirrhilabrus luteo</i>	1	1.59	.49	.49	.38
<i>Cirrhilabrus punctatus</i>	4	1.01	.48	.43	.49
<i>Cirrhilabrus ryuku</i>	1	1.73	.60	.49	.36
<i>Cirrhilabrus scottorum</i>	6	1.08	.47	.49	.46
<i>Clepticus parrae</i>	2	1.95	.68	.61	.36
<i>Coris aurilineata</i>	3	.69	.38	.52	.55
<i>Coris aygula</i>	5	.64	.38	.49	.59
<i>Coris batuensis</i>	3	.67	.36	.47	.51
<i>Coris dorsomacula</i>	3	.84	.44	.51	.52
<i>Coris gaimard</i>	5	.81	.40	.50	.50
<i>Coris pictoides</i>	3	.69	.43	.51	.61
<i>Cymolutes praetextatus</i>	4	1.26	.40	.55	.38
<i>Cymolutes torquatus</i>	5	1.03	.41	.52	.40
<i>Diproctacanthus xanthurus</i>	6	.76	.40	.59	.53
<i>Gomphosus varius</i>	6	1.15	.49	.58	.45
<i>Halichoeres biocellatus</i>	3	.83	.36	.57	.47
<i>Halichoeres bivittatus</i>	1	.46	.52	.76	.64
<i>Halichoeres chloropterus</i>	3	.73	.40	.48	.53
<i>Halichoeres chrysus</i>	4	.73	.41	.58	.54
<i>Halichoeres garnoti</i>	1	.78	.38	.58	.49
<i>Halichoeres hortulanus</i>	5	.97	.39	.55	.43
<i>Halichoeres maculipinna</i>	2	.88	.32	.57	.49
<i>Halichoeres margaritaceus</i>	4	.71	.36	.50	.51
<i>Halichoeres marginatus</i>	4	.85	.33	.58	.43
<i>Halichoeres melanurus</i>	4	.80	.38	.53	.48
<i>Halichoeres melasmapomus</i>	2	.90	.45	.52	.49
<i>Halichoeres miniatus</i>	4	.79	.42	.48	.53
<i>Halichoeres nebulosus</i>	2	.63	.38	.44	.60
<i>Halichoeres nigrescens</i>	4	.90	.42	.51	.47
<i>Halichoeres ornatissimus</i>	5	.85	.40	.58	.49
<i>Halichoeres pictus</i>	1	1.20	.50	.61	.43
<i>Halichoeres poeyi</i>	1	.84	.39	.58	.46
<i>Halichoeres prosopion</i>	6	.81	.42	.54	.54
<i>Halichoeres richmondi</i>	2	1.11	.39	.62	.45
<i>Halichoeres scapularis</i>	4	.90	.42	.53	.48
<i>Halichoeres trimaculatus</i>	6	.86	.41	.53	.49
<i>Halichoeres zeylonicus</i>	4	.77	.43	.55	.53
<i>Hemigymnus fasciatus</i>	3	.67	.32	.52	.53
<i>Hemigymnus melapterus</i>	4	.60	.33	.52	.53
<i>Hologymnosus annulatus</i>	9	.87	.40	.71	.46
<i>Hologymnosus doliatus</i>	4	.74	.39	.70	.52
<i>Labrichthys unilineatus</i>	5	.72	.37	.57	.54
<i>Labroides bicolor</i>	4	.55	.40	.74	.61
<i>Labroides dimidiatus</i>	6	.71	.39	.68	.54
<i>Labroides pectoralis</i>	4	.56	.38	.70	.59
<i>Labroides phthirophagus</i>	1	.79	.36	.68	.44
<i>Labropsis australis</i>	5	.60	.35	.59	.56
<i>Labropsis polynesica</i>	1	.86	.33	.61	.45
<i>Labropsis xanthonota</i>	4	.60	.34	.53	.58
<i>Leptojulius cyanopleura</i>	3	.82	.45	.56	.55

Table A1 (Continued)

Species	N	KT	Jaw	Nasal	Maxilla
<i>Macropharyngodon choati</i>	5	.81	.39	.43	.50
<i>Macropharyngodon kutieri</i>	4	.90	.41	.48	.47
<i>Macropharyngodon meleagris</i>	5	.67	.32	.44	.48
<i>Macropharyngodon negrosensis</i>	6	.84	.39	.45	.49
<i>Novaculichthys taeniourus</i>	5	.87	.39	.46	.49
<i>Oxycheilinus bimaculatus</i>	6	.75	.41	.49	.55
<i>Oxycheilinus digrammus</i>	22	.82	.44	.57	.51
<i>Oxycheilinus unifasciatus</i>	6	.73	.40	.55	.53
<i>Oxyjulis californica</i>	1	.99	.50	.74	.45
<i>Pseudocheilinus evanidus</i>	5	.78	.43	.47	.55
<i>Pseudocheilinus hexataenia</i>	5	1.18	.48	.46	.45
<i>Pseudocheilinus octotaenia</i>	7	.83	.49	.49	.55
<i>Pseudocoris yamashiroi</i>	4	.92	.53	.54	.57
<i>Pseudodax moluccanus</i>	4	.89	.42	.38	.49
<i>Pseudojuloides atavai</i>	1	1.09	.43	.73	.39
<i>Pseudojuloides cerasinus</i>	5	.83	.43	.68	.51
<i>Pseudolabrus guentheri</i>	4	.76	.39	.47	.54
<i>Pteragogus cryptus</i>	6	.84	.45	.45	.52
<i>Pteragogus enneacanthus</i>	3	.78	.39	.42	.52
<i>Stethojulis bandanensis</i>	3	.65	.34	.49	.53
<i>Stethojulis interrupta</i>	5	.70	.39	.55	.54
<i>Stethojulis strigiventor</i>	2	.55	.44	.60	.64
<i>Stethojulis trilineata</i>	6	.81	.37	.54	.46
<i>Thalassoma amblycephalum</i>	6	.92	.44	.47	.51
<i>Thalassoma bifasciatum</i>	2	.97	.42	.56	.44
<i>Thalassoma hardwicke</i>	4	.89	.41	.52	.46
<i>Thalassoma janseni</i>	4	.86	.38	.51	.45
<i>Thalassoma lucasanum</i>	2	1.00	.40	.55	.41
<i>Thalassoma lunare</i>	3	.82	.35	.44	.47
<i>Thalassoma lutescens</i>	4	.72	.36	.52	.51
<i>Thalassoma quinquevittatum</i>	6	.87	.39	.53	.47
<i>Thalassoma trilobatum</i>	3	.64	.37	.47	.56
<i>Wetmorella nigropinnata</i>	5	1.11	.57	.57	.48
<i>Xyphochelium typus</i>	4	.44	.31	.34	.68
<i>Xyrichtys aeneitensis</i>	3	.71	.23	.56	.38
<i>Xyrichtys martinicensis</i>	1	1.46	.40	.53	.32
<i>Xyrichtys novacula</i>	1	1.18	.34	.57	.33
<i>Xyrichtys pavo</i>	4	.67	.27	.62	.39
<i>Xyrichtys splendens</i>	2	1.25	.41	.61	.36

Note: Measures were taken on adult fish. Numbers indicate the mean value of the sampled individuals for each variable except where a single individual was measured. See Wainwright et al. 2004 for additional information on morphometric methods. N = number of individuals measured; KT = maxillary KT; jaw, nasal, and maxilla refer to four-bar element lengths expressed as a proportion of the fixed link (fig. 1).

## APPENDIX B



**Figure B1:** Calculation of maxillary KT. Maxillary KT describes the amount of rotation of the maxilla per degree of rotation of the lower jaw. The measure is a function of the lengths of the four-bar elements (fixed, lower jaw, nasal, maxilla), the starting angle, and the amount of input rotation. Essentially, maxillary KT is calculated as the ratio of change in maxilla rotation (angle  $z$ ) to lower jaw rotation (assumed in this study to be  $30^\circ$ ). Details of this calculation are provided as a Mathematica notebook.

## Literature Cited

- Alfaro, M. E., D. I. Bolnick, and P. C. Wainwright. 2004. Evolutionary dynamics of complex biomechanical systems: an example using the four-bar. *Evolution* 58:495–503.
- Baldwin, B. G., and M. J. Sanderson. 1998. Age and rate of diversification of the Hawaiian silversword alliance (Compositae). *Proceedings of the National Academy of Sciences of the USA* 95:9402–9406.
- Farrell, B. D. 1998. “Inordinate fondness” explained: why are there so many beetles? *Science* 281:555–559.
- Fontana, W., and P. Schuster. 1998. Shaping space: the possible and the attainable in RNA genotype-phenotype mapping. *Journal of Theoretical Biology* 194:491–515.
- Friel, J. P., and P. C. Wainwright. 1998. Evolution of motor patterns in tetradontiform fishes: does muscle duplication lead to functional diversification? *Brain, Behavior, and Evolution* 52:159–170.
- Gatz, A. J., Jr. 1979. Community organization in fishes as indicated by morphological features. *Ecology* 60:711–718.
- Grant, P. R. 1986. *Ecology and evolution of Darwin’s finches*. Princeton University Press, Princeton, NJ.
- Hulsey, C. D., and P. C. Wainwright. 2002. Projecting mechanics into morphospace: disparity in the feeding system of labrid fishes. *Proceedings of the Royal Society of London B* 269:317–326.
- Kelly, J. K. 2003. Deleterious mutations and the genetic variation of male fitness components in *Mimulus guttatus*. *Genetics* 164:1071–1085.
- Koehl, M. A. R. 1996. When does morphology matter? *Annual Review of Ecology and Systematics* 27:501–542.
- Kovach, I. S. 1996. A molecular theory of cartilage viscoelasticity. *Biophysical Chemistry* 59:61–73.
- Lande, R. 1979. Quantitative genetic analysis of multivariate evolution, applied to brain : body size allometry. *Evolution* 33:402–416.
- Lauder, G. V. 1990. Functional morphology and systematics: studying functional patterns in an historical context. *Annual Review of Ecology and Systematics* 21:317–340.
- Lewontin, R. 1978. Adaptation. *Scientific American* 239:157–169.
- Liem, K. F., and J. W. M. Osse. 1975. Biological versatility, evolution, and food resource exploitation in African cichlid fishes. *American Zoologist* 15:427–454.
- Lovette, I. J., E. Bermingham, and R. E. Ricklefs. 2002. Clade-specific morphological diversification and adaptive radiation in Hawaiian songbirds. *Proceedings of the Royal Society of London B* 269:37–42.
- Lynch, M. 1984. The selective value of alleles underlying polygenic traits. *Genetics* 108:1021–1033.
- Marvaldi, A. E., A. S. Sequeira, C. W. O’Brien, and B. D. Farrell. 2002. Molecular and morphological phylogenetics of weevils (coleoptera, curculionidea): do niche shifts accompany diversification? *Systematic Biology* 51:761–785.
- Middleton, K. M., and S. M. Gatesy. 2000. Theropod forelimb design and evolution. *Zoological Journal of the Linnean Society* 128:149–187.
- Muller, M. 1996. A novel classification of planar four-bar linkages and its application to the mechanical analysis of animal systems. *Philosophical Transactions of the Royal Society of London B* 351:689–720.
- Nishikawa, K. C. 1999. Neuromuscular control of prey capture in

- frogs. *Philosophical Transactions of the Royal Society of London B* 354:941–954.
- Norberg, U. M. 1994. Wing design, flight performance, and habitat uses in bats. Pages 205–239 in P. C. Wainwright and S. M. Reilly, eds. *Ecological morphology*. University of Chicago Press, Chicago.
- Ohta, T. 1992. The nearly neutral theory of molecular evolution. *Annual Review of Ecology and Systematics* 23:263–286.
- Orr, H. A. 1998. Testing natural selection vs. genetic drift in phenotypic evolution using quantitative trait locus data. *Genetics* 149:2099–2104.
- Ostrom, J. H. 1979. Bird flight: how did it begin? *American Scientist* 67:45–56.
- Phillips, P. C., M. C. Whitlock, and K. Fowler. 2001. Inbreeding changes the shape of the genetic covariance matrix in *Drosophila melanogaster*. *Genetics* 158:1137–1145.
- Powell, P., R. R. Roy, P. Kanim, M. A. Bello, and V. Edgerton. 1984. Predictability of muscle tension from architectural determinations in guinea pig hindlimbs. *Journal of Applied Physiology* 57:1715–1721.
- Ricklefs, R. E., and D. B. Miles. 1994. Ecological and evolutionary inferences from morphology: an ecological perspective. Pages 13–41 in P. C. Wainwright and S. M. Reilly, eds. *Ecological morphology*. University of Chicago Press, Chicago.
- SAS Institute. 2002. JMP. Version 5.01. SAS Institute, Cary, NC.
- Schaefer, S. A., and G. V. Lauder. 1986. Historical transformation of functional design: evolutionary morphology of feeding mechanisms in lorocarioid catfishes. *Systematic Zoology* 35:489–508.
- . 1996. Testing hypotheses of morphological change: biomechanical decoupling in lorocarioid catfishes. *Evolution* 50:1661–1675.
- Schluter, D. 1996. Adaptive radiation along genetic lines of least resistance. *Evolution* 50:1766–1774.
- . 2000. *The ecology of adaptive radiation*. Oxford Series in Ecology and Evolution. Oxford University Press, Oxford.
- Schuster, P., and W. Fontana. 1999. Chance and necessity in evolution: lessons from RNA. *Physica D: Nonlinear Phenomena* 133:427–452.
- Schuster, P., W. Fontana, P. F. Stadler, and I. Hofacker. 1994. From sequences to shapes and back: a case study in RNA secondary structures. *Proceedings of the Royal Society of London B* 255:279–284.
- Stadler, B. M. R., P. F. Stadler, G. P. Wagner, and W. Fontana. 2001. The topology of the possible: formal spaces underlying patterns of evolutionary change. *Journal of Theoretical Biology* 213:241–274.
- Taylor, C. R., and E. R. Weibel. 1981. Design of the mammalian respiratory system. I. Problem and strategy. *Respiration Physiology* 44:1–10.
- Toro, E., A. Herrel, and D. J. Irschick. 2004. The evolution of jumping performance in Caribbean *Anolis* lizards: resolution of a biomechanical trade-off? *American Naturalist* 163:844–856.
- Vermeij, G. 1973. Adaptation, versatility, and evolution. *Systematic Zoology* 22:466–477.
- Wainwright, P. C., D. R. Bellwood, M. W. Westneat, J. R. Grubich, and A. S. Hoey. 2004. A functional morphospace for the skull of labrid fishes: patterns of diversity in a complex biomechanical system. *Biological Journal of the Linnean Society* 82:1–25.
- Wainwright, S. A., W. D. Biggs, J. D. Curry, and J. M. Gosline. 1976. *Mechanical design in organisms*. Edward Arnold, London.
- Westneat, M. W. 1990. Feeding mechanics of teleost fishes (Labridae): a test of four-bar linkage models. *Journal of Morphology* 205:269–295.
- . 1995. Feeding, function, and phylogeny: analysis of historical biomechanics in labrid fishes using comparative methods. *Systematic Biology* 44:361–383.
- Westneat, M. W., M. E. Alfaro, P. C. Wainwright, D. R. Bellwood, J. R. Grubich, J. L. Fessler, K. D. Clements, and L. L. Smith. Forthcoming. Local phylogenetic divergence and global evolutionary convergence of skull function in reef fishes of the family Labridae. *Proceedings of the Royal Society of London B*.
- Winemiller, K. O. 1991. Ecomorphological diversification in lowland freshwater fish assemblages from five biotic regions. *Ecological Monographs* 61:343–365.
- Wolfram Research. 2002. *Mathematica 4.2*. Wolfram Research, Champaign, IL.
- Zuckerandl, E. 1997. Neutral and nonneutral mutations: the creative mix—evolution of complexity in gene interaction systems. *Journal of Molecular Evolution* 44:S2–S8.

Acting Editor: Raymond B. Huey